

# Design Guidelines for a Copper Halide Laser

---

Chapter 1	Introduction	pg. 2
Chapter 2	Principle of operation	pg. 3
Chapter 3	Copper-Halide laser parameters	pg. 4
Chapter 4	Electrical Circuit	pg. 12
Chapter 5	Tube design	pg. 17
Chapter 6	Example of laser construction	pg. 18
	Acknowledgement	pg. 20

## **Chapter 1 Introduction**

The copper vapor laser (CVL) is currently under intensive research and development in several laboratories. The laser combines the following advantages over other visible gas lasers <sup>(1)</sup>:

- High peak power, over 400 kW
- Over 1% efficiency
- Average power of tens of watts

The CVL field is split into two main branches. One is the development of lasers using “genuine” copper vapor <sup>(2-3)</sup>. Copper must be heated to 1500 to 1700°C in order to achieve a suitable vapor pressure. The other branch is development of lasers utilizing vapors of copper-bearing compounds, mainly the copper halides, CuCl, CuBr, CuI (Refs. 4-7). The copper halides have considerably higher vapor pressures than metallic copper. It is possible to achieve a sufficient copper concentration for lasing in the 300 to 600°C range (depending on the copper halide). However, for low repetition rate application, two electrical pulses are needed to create a single light pulse from a copper halide laser.

Although the rapid improvement in laser performance of the last few years is still continuing, the state of the art has advanced sufficiently to permit construction of reliable copper-halide lasers for various applications. Two such lasers are currently in use in our laboratory, one to pump a dye laser and the other for pulsed holography.

In chapter 2 we describe the principle of the longitudinal copper-halide laser and in chapter 3 we introduce the parameters governing its performance. Suitable electronic circuits are described in chapter 4. In chapter 5 we present the laser design. The performance of a double-pulse longitudinal copper-halide laser is presented in chapter 6.

## **Chapter 2 Principle of operation**

The laser consists of a vacuum-tight discharge tube which can be heated to the desired temperature and has appropriate windows for coupling the laser medium with the optical cavity. A buffer gas is introduced into the tube together with the copper halide. An external pulser excites the laser. At low repetition rates two pulses are necessary to achieve lasing. The first pulse provides copper atoms by dissociating the halide. The process is quite slow<sup>(8)</sup>. The second pulse is delayed until an adequate copper atom concentration has built up. Then a fast discharge pumps the copper atoms to the upper laser levels by electron collisions (see Fig. 1)

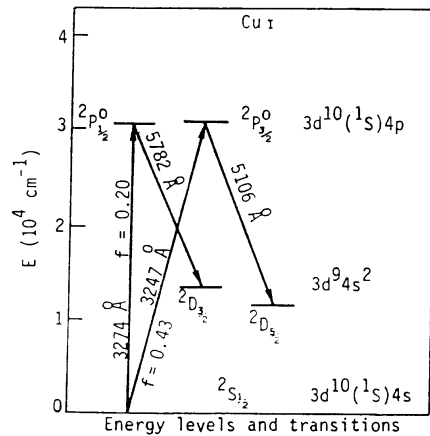


*Figure 1.* Energy levels and transitions of the copper atom.  $^2D$  is the lowest metastable state. The resonance transition is  $^2S \rightarrow ^2P$ .

Population inversion is enhanced by radiation trapping in the resonance transition. The CVL has a large gain so the population in the upper levels decays very rapidly by stimulated emission. The lower laser levels ( $^2D$ ) are metastable leading to self-termination of the laser action. Only the energy delivered to the laser prior to self-termination is usable for excitation. The copper halide then reforms by a slow recombination process, leading to cyclic operation.

## **Chapter 3 Copper-halide laser parameters**

The following parameters must be considered in the design of a copper-halide laser.

### **3.1 Halide temperature**

Typical dependence of laser output on halide temperature is shown in Fig. 2. There is a definite optimum temperature; for all three halides the optimum temperature corresponds to the same vapor pressure,  $\sim 0.1$  torr (Ref. 9). The optimum temperature is independent of other laser parameters and is  $370^\circ\text{C}$  for CuCl,  $420^\circ\text{C}$  for CuBr, and  $500^\circ\text{C}$  for CuI (Ref. 7).

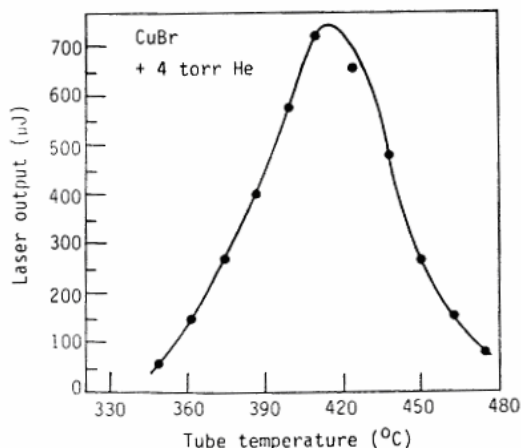


*Figure 2.* Dependence of laser output on tube temperature.

Dissociation energy: 2.8J;

Excitation energy: 2 J;

Tube length: 22 cm;

Tube diameter: 30 mm;

Delay: 300μs.

### **3.2 Buffer gas**

Buffer gas is essential in a laser in which the electrodes and windows are cold since it provides the discharge medium in the cold part of the tube and also prevents halide vapor from reaching and condensing on the windows. The buffer gas is the majority of species in the hot region as well. Argon, neon, and helium are suitable buffer gases; for low repetition-rate double-pulse operation we have found helium to give the best results.

Vetter and Nerheim found that a small quantity of HCl improves laser performance in a CuCl laser<sup>(10)</sup>.

Fig. 3 presents laser energy as a function of helium pressure for a CuBr laser. The curve is typical of all halides, with an optimum pressure of 3 to 5 torr, independent of tube diameter.

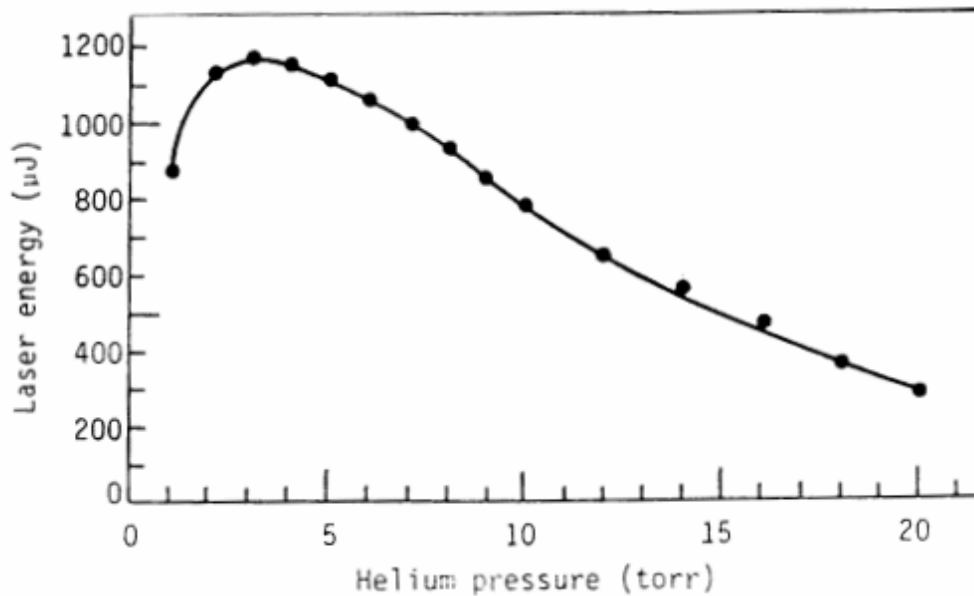


*Figure 3.* Dependence of laser output on helium buffer gas pressure. Tube length 22 cm, diameter 37 mm, Temperature: 430°C; Delay: 350μs; Dissociation energy: 6.4 J; Excitation Energy 5 J.

### 3.3 Delay

In order for lasing to occur the copper-halide molecules must dissociate to provide copper atoms<sup>(4)</sup>. The first electrical pulse in the double pulse laser causes dissociation; the second pulse excites the copper atoms. The delay time between the two pulses is an important laser parameter. Typical laser output as a function of delay time is shown in Fig. 4.

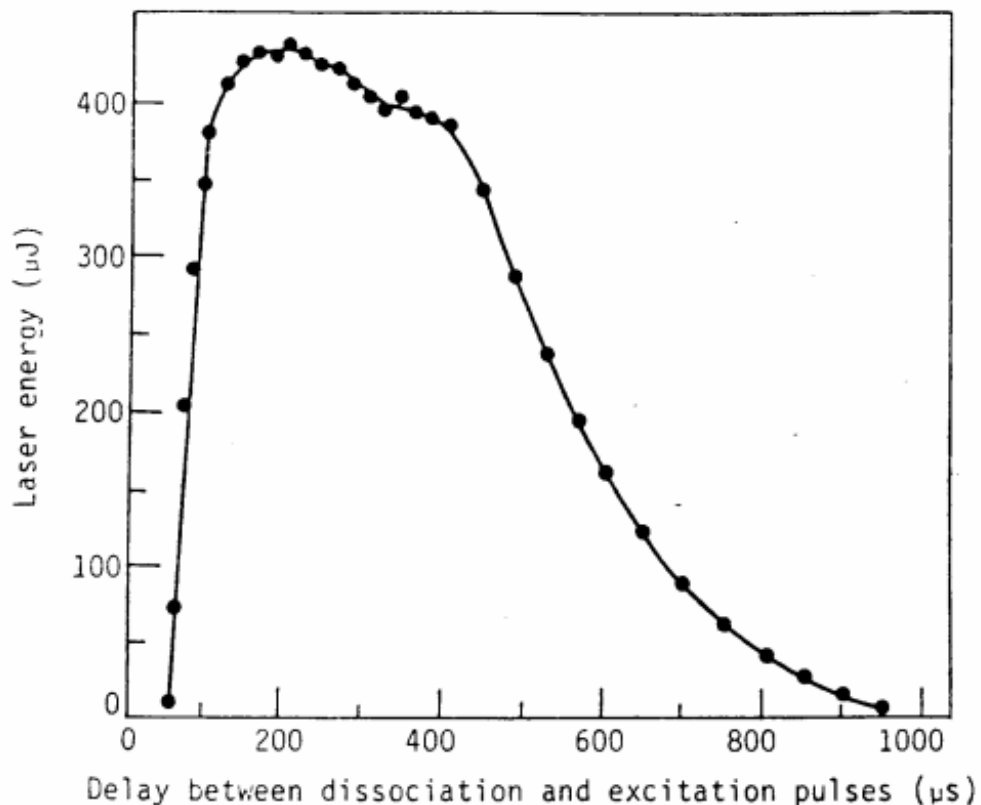


*Figure 4.* Dependence of laser output on delay between dissociation and excitation pulses. Tube length 22 cm, diameter 25 mm; Temperature: 430°C; He pressure: 4 torr; Dissociation energy: 2.4 J; Excitation energy: 2 J.

Figure 4 is characterized by three times:

- The minimum delay, prior to which lasing does not occur.
- The optimum delay, at which laser output is maximized.
- That maximum delay, after which lasing no longer occurs.

The ground-state copper-atom population builds up rather slowly after the dissociation pulse, then decays by recombination with the halogen atoms <sup>(8)</sup>. There is thus a maximum ground state population at some definite delay.

However, the experiments of Tenenbaum *et al.* <sup>(8)</sup> show that some population exists in the lower laser level, the metastable level, during the entire ground state build-up time. Maximum population inversion and laser output are achieved only when the metastable population decays, somewhat after the ground state population peak. This is the optimum delay time.

The minimum and optimum delay times are essentially independent of halide species if other parameters are held fixed. However, the maximum delay increases from CuCl to CuBr to CuI, reflecting differences in recombination rates.

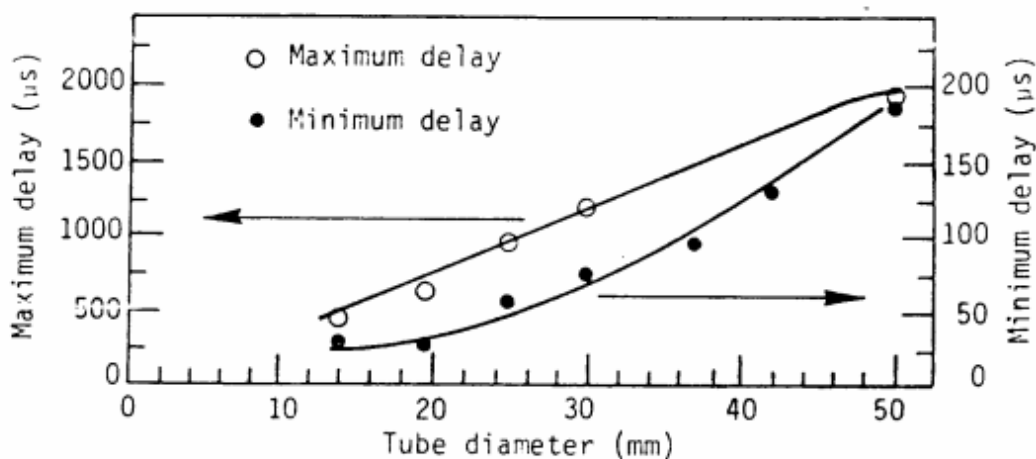


Figure 5. Minimum and maximum delays as a function of tube diameter. For each tube diameter the other parameters were chosen to maximize laser output.

### 3.4 Dissociation and excitation

Since most of the ground state copper atoms are created after completion of the first electrical pulse (8) and stimulated emission occurs on the leading edge of the second pulse, the width of the dissociation pulse is not very important whereas the excitation pulse should be as short as possible.

Fig. 6 is a basic schematic circuit of a capacitor discharge into a laser tube.

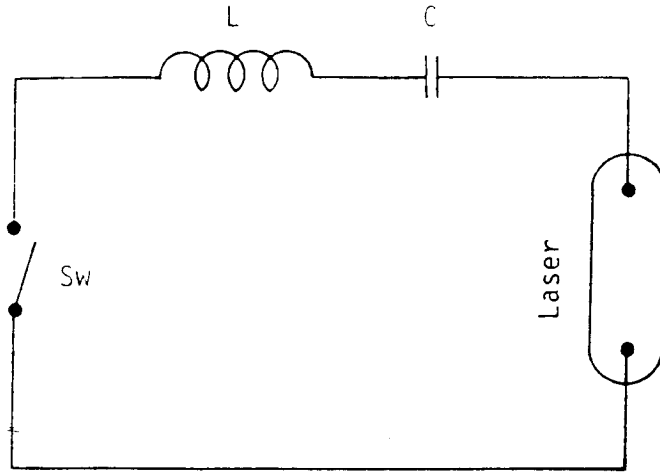


Figure 6. Schematic diagram of a capacitor discharge into laser tube. L represents parasitic inductance of the circuit and Sw represents the thyatron.

To a first approximation the discharge time is given by

$$t = p\sqrt{LC} \quad [1]$$

For a given energy

$$E = \frac{1}{2}CV^2 \quad [2]$$

or

$$t = p\sqrt{2LE} \quad V^{-1} = K_1V^{-1} \quad [3]$$

where  $K_1$  is a constant. For small  $t$ ,  $V$  must be large. Fig. 7 shows that a laser excited by discharging a 10 nF capacitor gives higher output than with a 25 nF capacitor for the same excitation energy, i.e. the output increases with excitation voltage or decreases with rise time.

Suppose the available excitation energy is given by

$$E_1 = E \frac{t}{\tau} \quad [4]$$

where  $t$  is the excitation pulse width and  $\tau$  is the time until lasing occurs.



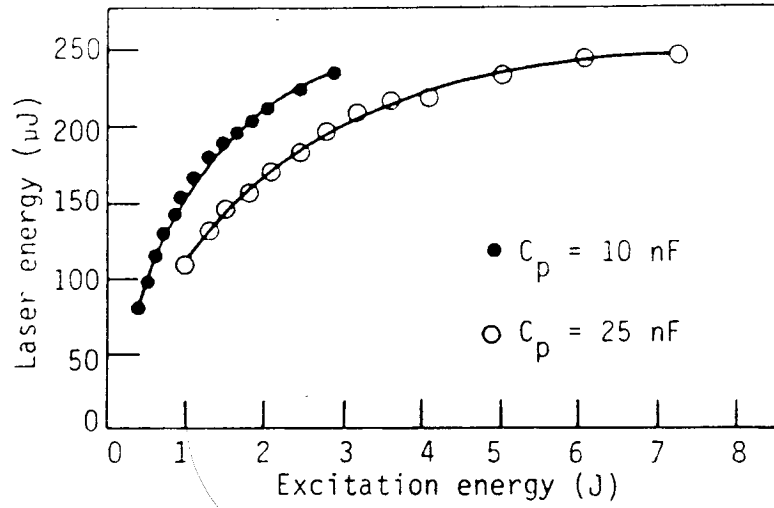


*Figure 7.* Laser output energy as a function of excitation energy for two different excitation capacitors. Tube length 22 cm, diameter 19.5 mm; Temperature: 430°C; He pressure: 3 torr; Delay: 140μs; Dissociation energy: 720 mJ.

Then for two different capacitors  $C_1$  and  $C_2$  with two pulse widths  $t_1$  and  $t_2$ , respectively we have

$$\frac{E_2}{E_1} = \frac{Et/t_2}{Et/t_1} = \frac{t_1}{t_2} = \left( \frac{C_1}{C_2} \right)^{1/2} \quad [5]$$

If the laser output is linear with available input energy  $E_i$ , agreement between Eq.[5] and Fig. 7 is quite good.

Laser energy as a function of dissociation energy is described in Fig. 8. The output energy is dependent on dissociation energy but not on capacitance. A remarkable difference between dissociation and excitation requirements is that there is an optimum dissociation energy but no optimum excitation energy, although laser output does saturate with excitation energy.

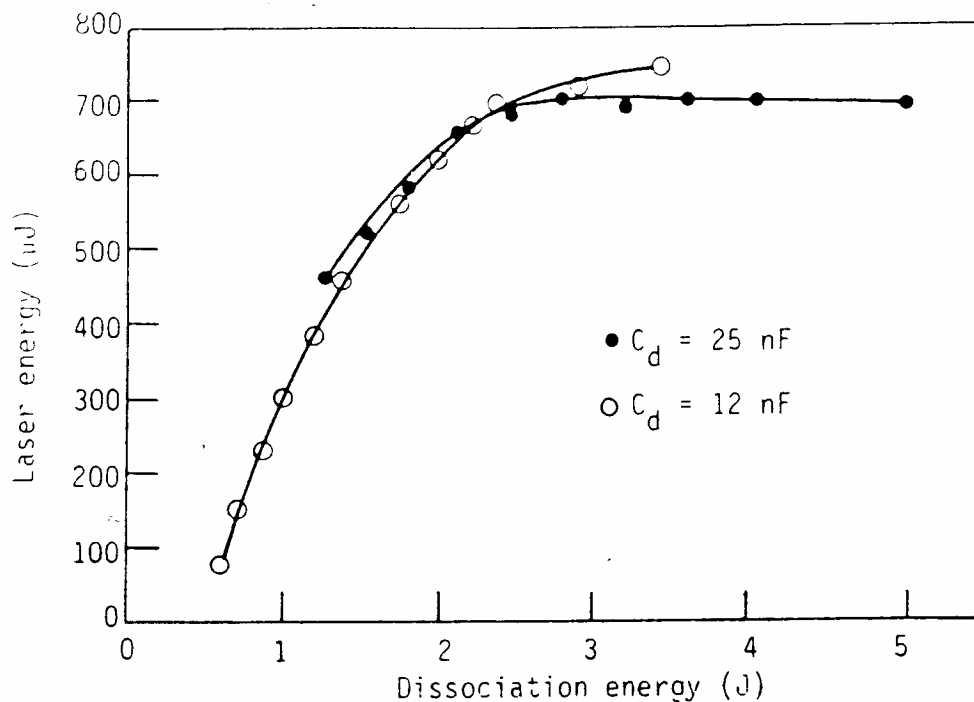


*Figure 8.* Laser output energy as a function of dissociation energy for two different dissociation capacitors. Tube length: 22 cm, diameter 30 mm; Temperature: 430°C; He pressure: 4 torr; Delay: 300  $\mu$ s; Excitation energy: 2 J.

### 3.5 Tube diameter

Since there is an optimum laser temperature, the output can only be increased by increasing tube volume. Fig. 9 presents laser output as a function of tube cross section (tube diameter). Optimum delay and excitation and dissociation energies were found for each tube diameter, while all other parameters were held constant. The appropriate energies for each diameter are presented in table 1. Since lasing depends not only excitation energy but capacitance, table 1 presents results for two different capacitances. For a given capacitance optimum dissociation energy increases with tube diameter, due to larger quantity of molecules to be dissociated. The excitation energy to reach saturation is independent of diameter (or even decreases slightly with increasing diameter).

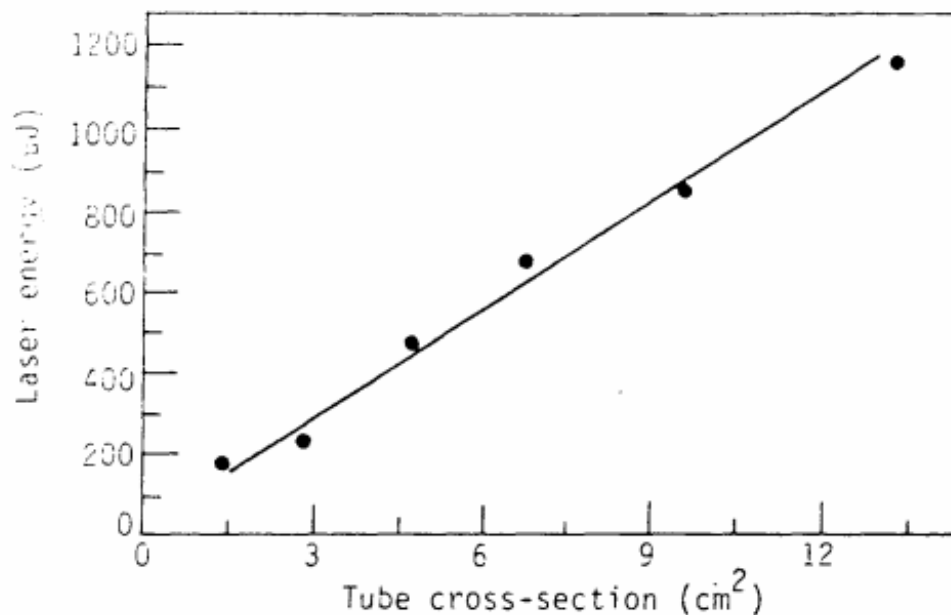


Figure 9. Dependence of laser output energy on tube cross-section (tube volume). The operating parameters for each cross-section were chosen to maximize laser output energy.

Table 1.

Appropriate dissociation and excitation energies for various tube diameters. “EX” denotes values obtained by extrapolation.

Tube diameter (mm)	Dissociation energy (J)		Excitation energy (J)	
	$C_d = 10 \text{ nF}$	$C_d = 25 \text{ nF}$	$C_p = 10 \text{ nF}$	$C_p = 25 \text{ nF}$
14.0	0.55	--	2.2	4.0
19.5	0.75	--	2.0	3.5
25.0	1.50	2.0	2.0	3.5
30.0	2.50	3.0	1.7	3.0
37.0	3.0 (EX)	3.2	1.5	2.5
42.0	4.5 (EX)	5.0	1.7	2.75

## **Chapter 4 Electrical Circuit**

The most critical element in the discharge circuit is the switch, which must hold off 20 to 50 kilovolts and conduct several kiloamperes with a rise time of a few nanoseconds. A straightforward double-pulse generator is described in Fig. 10.

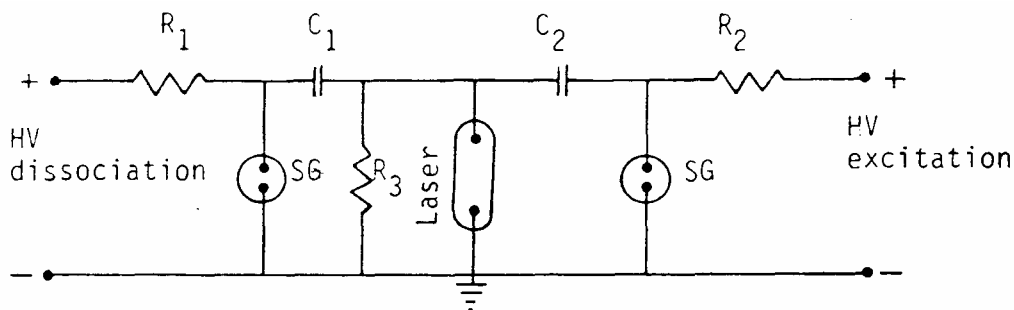


*Figure 10.* Schematic diagram of double-pulse generator for halide laser using resistive charging.

Spark gaps switch the energy stored in the dissociation and excitation capacitors into the laser tube. Since the recovery time of a spark gap is usually several milliseconds and the delay between the two pulses is tens or hundreds of microseconds, separate spark gaps must be used for the two pulses. The use of two spark gaps dictates the use of two capacitors. As a result the dissociation and excitation capacitances and voltages can be optimized separately. Spark gaps have an advantage over thyratrons in this configuration since they are triggered by high voltage pulses and are immune to prefiring as a result of high  $dV/dt$  on the anode. In addition no heater supply is required. On the other hand, the absence of a hot cathode increases the rise time and jitter. Hydrogen thyratrons have shorter rise times and much smaller jitter than spark gaps but are not as noise immune. Prefiring of thyratrons in a low repetition rate copper halide laser can be overcome by utilizing the following considerations:

- The main difficulty is firing of the excitation thyatron by the dissociation thyatron. The dissociation thyatron is not fired by the excitation thyatron since its capacitor has not yet recharged at the time of the excitation pulse.
- Since dissociation can be achieved by a slow, low-voltage pulse, an inductor in series with the dissociation thyatron can eliminate prefiring<sup>(7)</sup>.

The circuit in Fig. 10 is inefficient both in components and in energy (resistive charging) and is incapable of achieving a high repetition rate. These problems can be overcome by using resonant charging (Fig. 11), although it is more difficult to optimize simultaneously dissociation and excitation pulses. Resonant charging also minimizes the number of high voltage points in the circuit.

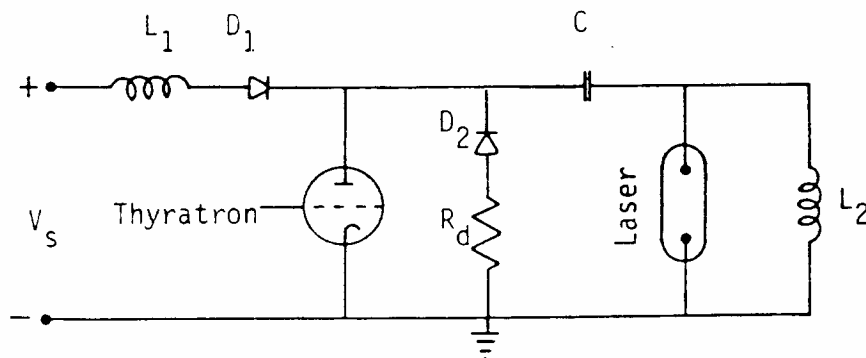


*Figure 11.* Schematic diagram of resonant charging circuit which permits the capacitor C to be charged to twice the power supply voltage (or more, depending on matching between discharge circuit and plasma tube).

The discharge circuit itself is oscillatory in nature (see Fig. 6) and if it is not heavily damped by the laser tube two undesirable phenomena occur:

- The energy available for laser excitation is reduced.
- Capacitor C is charged to a much higher voltage than  $2V_s$  ( $V_s$  is the supply voltage) and the capacitor, thyatron or hold-off diode can be damaged.

The classic solution of clamping diode and dissipation resistor ( $D_2$  and  $R_d$  in Fig. 11) protects the circuitry but wastes energy.

Best results are obtained when the laser tube is matched to the discharge circuit,

$$R = \sqrt{L/C} \quad [6]$$

where  $R$  is the effective tube resistance during the discharge,  $L$  is the total discharge circuit inductance and  $C$  is the storage capacitance. Since the pulse width is given approximately by  $t = p\sqrt{LC}$ , for a matched circuit we have

$$t = pRC \quad [7]$$

This equation should be the starting point of the laser circuit design.

The circuit components of Fig. 11 must be selected carefully. Since dissociation and excitation energies cannot be both equal and simultaneously optimized, we compromised by charging the capacitor to an energy which is the average of the two optima. Values of the optimum energies are given in table 1 as a function of tube diameter (tube cross-section).

For maximum discharge slew rate, the highest technically permitted voltage should be used. This voltage,  $V_m$ , is given by the smaller of the capacitor or thyatron breakdown voltage. The needed capacitance is then calculated from

$$C = \frac{2E}{V_m^2} \quad [8]$$

where  $E$  is the energy chosen above.

The delay between dissociation and excitation is 100 to 300  $\mu\text{s}$  for the conditions described above. During this time the capacitor must be recharged to deliver the excitation pulse. Denoting this time by  $t_{\min}$ , this condition can be expressed as

$$t_{\min} > p\sqrt{LC} \quad [9]$$

Discharge of capacitor C through the thyatron causes a current to develop in  $L_1$  with an initial slope  $V_s/L_1$ . The thyatron will conduct this current until it recovers. Care should therefore be taken that the current not reach  $I_h$ , the thyatron hold current, during the thyatron recovery time  $\Delta t$ .  $L_1$  should therefore also obey the relation.

$$L_1 > \frac{V_s \Delta t}{I_h} \quad [10]$$

Equation [9] and [10] also imply that

$$\frac{p_2 C \Delta t}{t_{\min}} < I_h \quad [11]$$

For a given thyatron  $I_h$  is not under the control of the user and  $V_s$ , C and  $t_{\min}$  are already fixed. So, unless the thyatron recovery time  $\Delta t$  is short enough the thyatron will be latched in a conducting mode, preventing capacitor charging. Recovery is completed when the volume between the thyatron anode and the grid is de-ionized. The sooner this is accomplished, the shorter  $\Delta t$ . Since ions recombine mainly on the grid, a negative bias from a low-impedance source enhances recovery by permitting a large recombination current. In addition, reduction of the reservoir voltage reduces the hydrogen pressure in the thyatron, reducing the time for ion diffusion to the grid.

Fig. 12 describes a grid circuit in which the trigger and bias circuits are separated in order to minimize the recovery impedance.

The recombination current is drawn from the bias supply and is about half the average current through the thyatron anode.

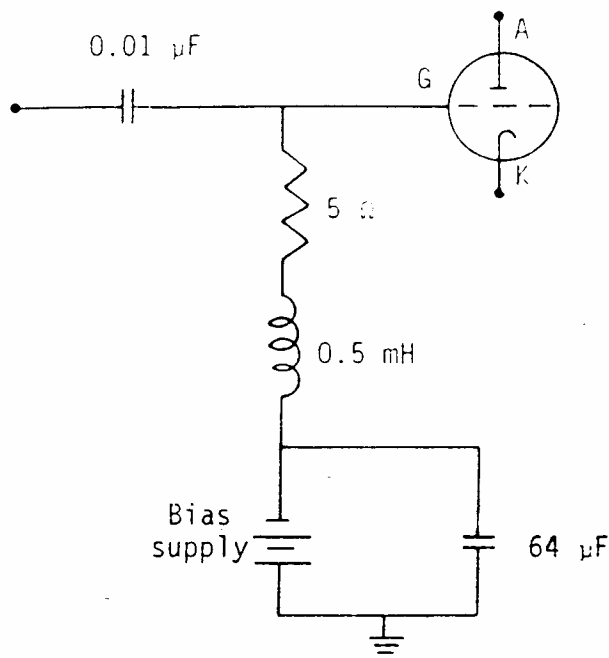


*Figure 12.* Grid circuit designed to minimize recovery impedance.

Some inexpensive surplus glass thyratrons are suitable for the circuit. Using the biasing method of Fig. 12 we have successfully operated a 5948A glass hydrogen thyatron with  $V_S = 8 \text{ kV}$  and  $L_1 = 0.3 \text{ H}$ .  $L_2$  is approximately  $100 \mu\text{H}$ , which is the inductance required to complete the charging circuit without reducing its  $Q$ . Its effect on the discharge is negligible.



## **Chapter 5 Tube Design**

Since the copper halides reach the required vapor pressure only at temperatures of several hundred degrees Celsius, a sealed off tube must be heated throughout, including the windows and electrodes.

Although this approach is feasible, we prefer the easier method of cold electrodes and windows. In such a laser the halide migrates continuously from the hot to the cold zone, depleting the halide reservoir in the active zone. In addition the halide solidifies in the cold zone, reducing the tube aperture. In order to ease these problems we designed the tube shown schematically in Fig. 13. The center (active) zone of the tube includes some 'pockets' containing about 20 grams of halide, which is sufficient for about 50 hours of operation. The condensed material accumulates in the widened regions, outside the active laser aperture. The tube can be refilled easily by removing the windows; its operating life is many hundreds of hours.

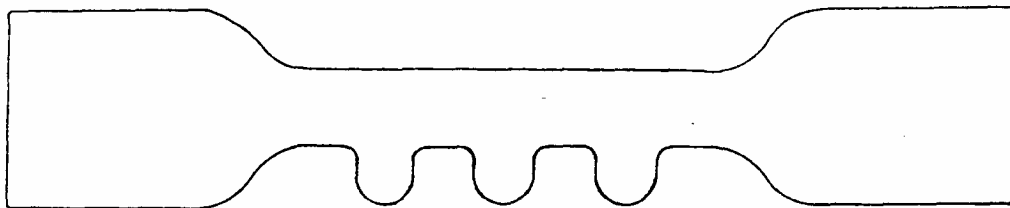


*Figure 13.* Schematic representation of a laser tube design to maximize operating time.

## **Chapter 6 Example of laser construction.**

The laser tube is a pyrex tube blown similarly to that of Fig. 13. The inner diameter of the narrow section is 25 mm and its length is 340 mm, the overall tube length is 700 mm and the heated zone length is 400 mm. The tube is joined at both ends to water cooled electrodes by means of O-rings (Fig. 14). The electrodes also support the Brewster angle windows. The cooling water arrangement is shown in Fig. 14. Tap water enters the cooling passages in the electrodes through ¼" polyethylene tubes. Electrical conduction through the cooling tubes is negligible. The anode is grounded; the vacuum pump is connected to that side of the tube. The gas handling system is also shown in Fig. 14. It is designed to maintain a pressure of 5 torr helium while slowly replacing the buffer gas. The gas enters the tube near the windows and protects them from halide 'dust'. The center zone of the laser is heated by a 3" split furnace (Applied Test Systems Series 3210) controlled by a variable transformer. The tube temperature is measured by a chromel-alumel thermocouple and a floating galvanometer. For CuBr the optimum temperature was found to be 420°C.

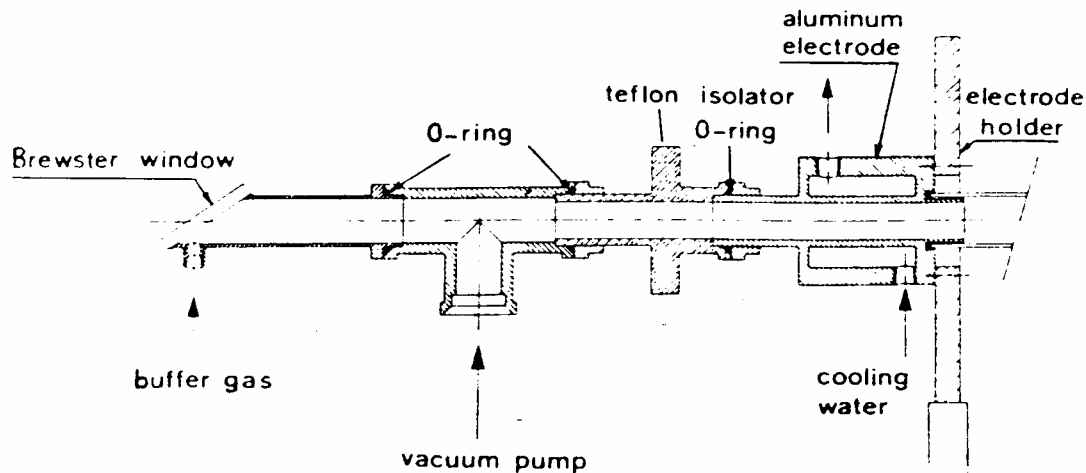


*Figure 14.* Schematic diagram of cooled electrode, gas inlet, and vacuum connection of CuBr laser.

The excitation circuit is that of Fig. 11 with the following components: The charging reactor is a 300 mH air-core reactor wound on a plastic core divided into three sections. The reactor is wound with 0.55 mm enamel-coated wire with mylar insulation between

layers. The complete assembly is placed in an insulating container filled with transformer oil. Other components are an EDI Model KHP-50 charging diode, four 1 nF (40 kV) capacitors in parallel and a 5948A glass thyatron with a 150 V bias and about a 1 kV trigger pulse. The interpulse separation was chosen to be 140  $\mu$ s. The optical cavity consists of a plane dielectric full reflector and a plane 8% output coupler.

With an 8 kV supply voltage the laser delivers 0.5 mJ pulses at a rate up to 120 Hz (60 mW average power). 80% of the power is in the green line (510.6 nm), the remainder in the yellow line (578.2 nm). The pulse duration is about 20 ns; hence peak power is 25 kW. Above 120 Hz the heat produced by the discharge cannot be neglected and the oven power must be reduced accordingly.

The laser is constructed from components which are readily available; its construction is straightforward. It makes available to modestly equipped laboratories a laser with output of up to 1 mJ/pulse at up to 100 pulses per second.

## **Acknowledgement**

We wish to thank H. Cohen for his technical assistance in many phases of the project.

## **Additional information**

This document was transcribed by myself, Jeff Aust, from a photocopied document I purchased from Information Unlimited located in Amherst, New Hampshire. I make no claims to accuracy though I believe my transcription is reasonably accurate. Some information appears to be missing in the photocopy document I have, most notably the references (Refs.) to other documents and footnote information. I do not have that information.

Please let me know of any errors you may find by sending an email to me at **cynblvd@yahoo.com**. **IMPORTANT: Please put the word laser in the subject of the email otherwise you may get filtered by my spam filters.** No copyright appears on the original so I don't know who owns the rights to this information.